Energy 238 (2022) 121761

Contents lists available at ScienceDirect

Energy

journal homepage: www.elsevier.com/locate/energy

Light and thermal management of the semi-transparent radiative cooling glass for buildings

Bin Zhao [a], Chuyao Wang [a], Mingke Hu [b], Xianze Ao [a], Jie Liu [a], Qingdong Xuan [c, **], Gang Pei [a, *]

[a] Department of Thermal Science and Energy Engineering, University of Science and Technology of China, Hefei, 230027, China
[b] Department of Architecture and Built Environment, University of Nottingham, University Park, Nottingham, NG7 2RD, UK
[c] School of Automotive and Transportation Engineering, Hefei University of Technology, 193 Tunxi Road, Hefei, 230009, China

ARTICLE INFO

Article history:
Received 2 June 2021
Received in revised form
26 July 2021
Accepted 8 August 2021
Available online 11 August 2021

Keywords:
Spectral selectivity
Radiative cooling
Transparent envelope
Building energy saving
Glass coating

ABSTRACT

Transparent envelopes account for a large amount of energy consumption of buildings, especially in hot climate regions. Glass is one of the main materials in transparent envelopes, so modifying the radiative properties of the glass is an alternative way for building energy saving. Here, a semi-transparent radiative cooling (ST/RC) glass was proposed by integrating the selective utilization of solar energy and passive radiative cooling. Comparative experiments based on two small-scale boxes were performed, which shows that the indoor air temperature of the box with the ST/RC glass is lower than that with the ordinary glass and the maximum temperature difference reached 16.4 °C, indicating that ST/RC glass can reduce the waste heat generated in the indoor environment. Besides, the daylighting level with the ST/RC glass is decreased by approximately 2/3 to support comfortable daylighting. Moreover, large-scale modeling of the building located in the Maldives was conducted and results show that the energy consumption of building could be saved by 21%–66.5% when the glass is modified to transmit visible light, reflect other solar irradiance, and emit like a blackbody, which indicates that the strategy of using light and thermal management of glass has the potential to reduce the energy consumption of buildings.

1. Introduction

Buildings consume more than 30 % of total energy use and this percentage is still in the increasing trend [1–3]. Space cooling, ventilation, heating, and lighting are four main contributors to the total building energy consumption, the proportions of which also vary with different climate regions. In hot climate regions, most energy consumption in the building sector is used for cooling. For example, it was reported that space cooling loads account for 32 % of the city's total electricity consumption in Hong Kong [4]. Hence, tailoring the energy behavior of the building envelopes, such as roof and window, to enhance building energy saving potential has been one of these areas' priority tasks.

The energy balance of a building is relevant to the sun (~5800 K), the universe (~3 K), and the ambient environment (~300 K). The heat gained by the building is mainly from sunlight by the radiative heat exchange between the buildings and the sun. The accumulated heat of the building is dissipated into the ambient environment and the universe by convection and radiative cooling. Radiative cooling is a passive cooling method that cools objects by radiating heat into the cold universe, which mainly relies on the transparency of the atmospheric window (AW) that ranges from 8 to 13 μm [5–8]. Thermodynamically, the sun and the universe are the ultimate heat source and sink of the earth, which plays an essential role in the energy balance of the buildings. Thus, modulating the radiative properties, including solar absorptivity and thermal emissivity, of the exterior surfaces exposed to the sunlight and sky directly is one of the key solutions to reduce the waste heat and saving energy for buildings.

Cool roofs are one of the promising spectral modulation strategies for buildings, which effectively manage the light and thermal reaction among the sun, universe, and ambient environment [9–11]. An ideal cool roof needs to be strongly solar reflective and exhibits high thermal emissivity in the infrared wavelength region, resulting in a minimum heat gain and maximum radiative cooling.

* Corresponding author.
** Corresponding author.
E-mail addresses: qingdongxuan@hfut.edu.cn (Q. Xuan), peigang@ustc.edu.cn (G. Pei).

https://doi.org/10.1016/j.energy.2021.121761
0360-5442/

Gentle et al. [9] developed a polyethylene mesh and showed that it can be applied in the cooling roof coupled with radiative cooling, which can reduce the heat gain of the building. Besides, this group also proposed a polymer surface to act as the open roof and demonstrated that the roof can remain a sub-ambient phenomenon throughout a hot summer day including under the peak solar irradiance of 1060 W m^{-2}, with an ambient temperature of 27 °C and infrared atmospheric intensity of 400 W m^{-2} [10]. Boixo et al. [11] predicted that a large-scale implementation of cool roofs in Andalucía can potentially save electricity of 295,000 kWh per year, which is approximately 2 % of the overall residential electricity consumption, showing the potential energy saving performance of the cool roofs. Besides of cool roofs, using commercial white paints [12–15] (e.g., titanium dioxide-based paint) on the external wall of buildings is also a useful way to reduce the solar power absorption due to the high solar reflectivity of the white paint. Ruan et al. experimentally demonstrated that $BaSO_4$ paints [12] and $CaCO_3$ paints [13] can achieve sub-ambient radiative cooling and these materials can be applied in building for energy saving. Moreover, Mandal et al. [14] predicted that spectrally selective paint is the preferred candidate for radiative cooling applications in buildings since paint material can be fabricated with a large scale and mature technology.

Importantly, on the other hand, optimizing the spectral properties of the glass is another important way to reduce the heat gain of buildings since approximately half the buildings' cooling load is caused by the sunlight transmitted through the glass, especially for buildings in hot climate regions [16–18]. Based on this consideration, several highlighted techniques appear to contribute, such as electrochromic windows [19–21] and spectrally selective windows [22]. For example, low-emissivity (Low-E) glass is an energy-saving glass for buildings [23–26], which reduces the infrared sunlight transmission and simultaneously maintains a high visible light transmission. Besides, the low emissivity (i.e., high reflectivity) spectrum of the Low-E glass can cause a local greenhouse effect and keep the indoor temperature at a stable condition. Abundiz-Cisneros et al. [23] proposed an aluminum-based Low-E filter for glass, which reduces the cost of the traditional silver-based Low-E coating while maintaining good optical properties for building energy saving. On the application scale level, Somasundaram et al. [24] analyzed the building energy-saving potential of the Low-E coating-based retrofit double glazing for tropical climate. The results showed that the Low-E coating-based double glazing can lead up to 4 % annual energy savings when installed on clear glass for tropical climate and the implementation of Low-E coating-based double glazing can reduce the mean radiant temperatures of the indoor environment and increase the thermal comfort of the occupants. Besides, this type of Low-E coating-based double glazing can be applied by combination with a solar film to further improve the energy-saving efficiency [26]. Although Low-E glass can saving energy for buildings, the temperature of the glass may be always higher than the indoor air temperature in hot climate regions, which will increase the cooling load of the building. Thus, enhancing the radiative cooling performance of the glass exterior surface is a good solution to reduce the glass temperature. Motivated by this idea, a metamaterial film with selectively solar transmittance and selectively high emissivity in the AW is developed and applied on roof glazing to reduce the cooling load of the building [27]. A case study showed that the annual air conditioning energy consumption of the referenced building can be reduced by 40.9 %–63.4 % in different conditions. However, selective high thermal emission just within the AW is not the perfect choice for roof glass radiative cooling in buildings since the transient temperature of the glass is higher than the ambient temperature during most of the day. Broadband thermal emitter is preferable under above-ambient radiative cooling because it can provide more cooling power than that of the selective thermal emitter.

Based on the above analysis, a strategy of light and thermal management of the glass for buildings based on the semi-transparent radiative cooling (ST/RC) glass is proposed to further save the electricity consumption of the building and reduce carbon dioxide emission. The light management of the glass means the glass needs to reflect near-infrared sunlight to reduce the waste heat generation of the indoor environment and simultaneously transmit the visible light for daylighting, but the transmitted light can't dramatically affect the thermal condition of the indoor environment, otherwise, additional HVAC load will be required. Besides, the thermal management of the glass means the glass needs to have strong broadband thermal emissivity to maximally dissipate waste heat. Compared with the existed spectrally selective glass (e.g., Low-E glass and transparent radiative cooling glass), not only radiative cooling mechanism is well integrated into the ST/RC glass, which fully explores the thermodynamic potential of the cold universe for building thermal management, but also the visible light transmittance of the glass is considered for both daylight and space cooling/heating.

In this paper, a semi-transparent solar film is applied to the glass to reduce its solar transmittance to reduce waste heat generation while still keep the transmittance of visible light at a reasonable range for daylighting. Besides, a transparent radiative cooling film is also applied to the glass external surface to enhance its broadband thermal emissivity so that more heat of the glass can be pumped outside by radiative cooling. Comparative outdoor experiments based on two small-scale building boxes were conducted to evaluate the light and thermal management performance of the proposed glass structure for buildings. Furthermore, the energy-saving performance of the strategy using light and thermal management of glass is numerically predicted on a large scale based on the glass with perfect spectral selectivity.

2. Experimental section

2.1. Semi-transparent radiative cooling glass

The semi-transparent radiative cooling (ST/RC) glass includes an ordinary glass, a semi-transparent (ST) solar film, and a transparent radiative cooling (RC) film. The schematic of the ST/RC glass is shown in Fig. 1a. It can be found from Fig. 1b that the ST film is semi-transparent with a strong reflection effect, while RC film and ordinary glass are transparent. Notably, there is no additional film on the bare case, just ambient air. To characterize the optical properties of the glass, ST, and RC film, spectral transmittance and reflectance were measured. The solar transmittance and solar reflectivity of the glass and glass with ST solar film were measured using a spectrophotometer (SolidSpec-3700, Shimadzu) with a spectral resolution of 1 nm. The spectral transmittance and reflectivity of the glass and glass with transparent RC within the mid-infrared wavelength region were measured by a Fourier transform infrared spectrometer (Nicolet iS50, Thermo Fisher Scientific) coupled with a transmittance attachment and a gold-coated integrating sphere. Then, the spectral emissivity of the glass and glass with transparent RC was obtained using the energy balance law and Kirchhoff's law.

As shown in Fig. 2a, the ordinary glass shows a high transmittance within the solar radiation band, while the glass with the ST solar film has a relatively low solar transmittance. Notably, the transmittance of the glass with the ST solar film within the visible light region is higher than that within the near-infrared wavelength band, which can maintain the daylighting function of the glass for buildings in hot climate regions where the solar irradiance is

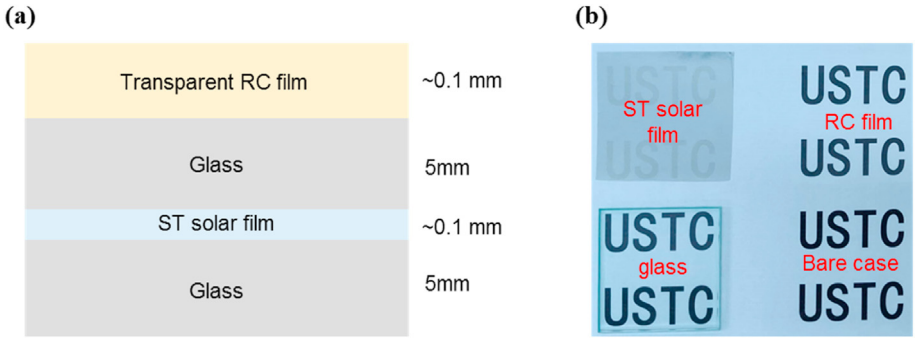

Fig. 1. Schematic of the ST/RC glass and the photo of the ST solar film, transparent RC film, and ordinary glass.

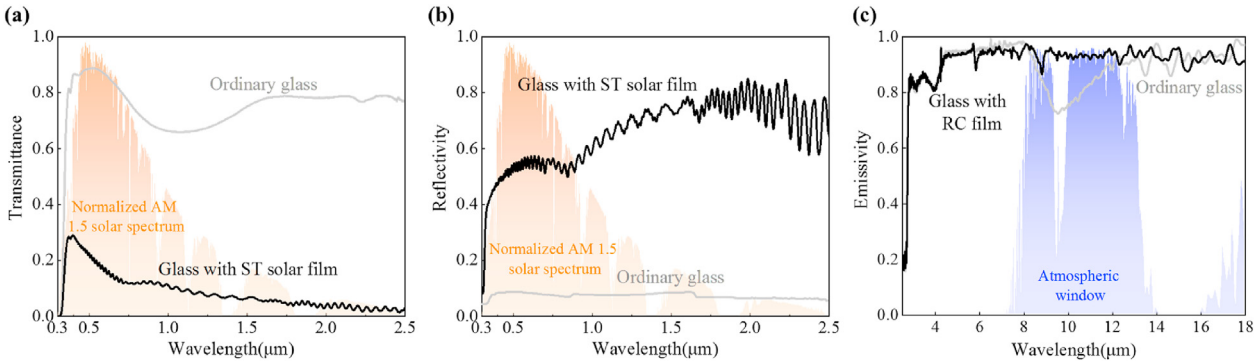

Fig. 2. (a) Measured spectral transmittance and (b) measured spectral reflectivity of the ordinary glass and glass with ST solar film with normalized AM 1.5 solar spectrum plotted as reference. (c) Measured spectral emissivity of the ordinary glass and glass with transparent RC film with an atmospheric transmittance curve plotted as reference.

always strong. Importantly, the glass with the ST film has a high solar reflection within the solar radiation band, especially within the near-infrared wavelength band (Fig. 2b), which means the surplus solar radiation can be reflected by the glass and the temperature of the glass can be maintained at a normal level. Fig. 2c depicts the emissivity of ordinary glass and glass with transparent RC film. It can be seen that the ordinary glass has an emissivity drop within the atmospheric window due to the phonon–polariton resonances of silica material [28,29], which will reduce the net emissive power of the glass. After covering the glass with the transparent RC film, the emissivity of the glass is improved significantly, which will increase the heat dissipation power of the glass to reduce its temperature when the glass is heated by the sunlight.

2.2. Outdoor experimental setup and measurement setting

Two identical small-scale box models are designed and fabricated for experimental testing. As shown in Fig. 3a, the wall and floor of the box are made of wood, and XPS thermal insulation materials are attached to the internal surface of the wall and floor. The surface of XPS is covered with reflective aluminum foil. The thickness of the wood wall/floor and XPS material are 15 mm and 18 mm, respectively. The length, width, and height of the box are 400 mm, 350 mm, and 450 mm, respectively, the photo of which is shown in Fig. 3b. Besides, 10-mm-thick ordinary glass and semi-transparent radiative cooling glass are attached on the top of two boxes to act as the only window, and we will refer to the former and latter as “ordinary case” and “modified case”, respectively.

The measurement setting of the experiment is shown in Fig. 4. Three T-type thermocouples (i.e., T_1, T_2, and T_3) are fixed in the indoor environment of the box with an aluminum foil-coated plastic stick to measuring the temperature of indoor air. The distance of the adjacent thermocouples is approximately 130 mm. The distance between the thermocouples T_3 and bottom XPS is about 78 mm. The illuminometer (RS-GZ-V05-2) is fixed on the south wall of the box to monitor the illuminance, which is powered by a power

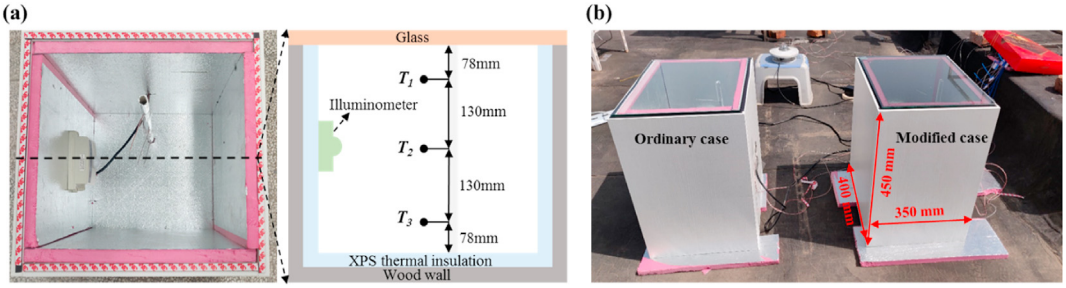

Fig. 3. (a) Top-view and schematic of section-view of the box model. (b) the photo of the two box models.

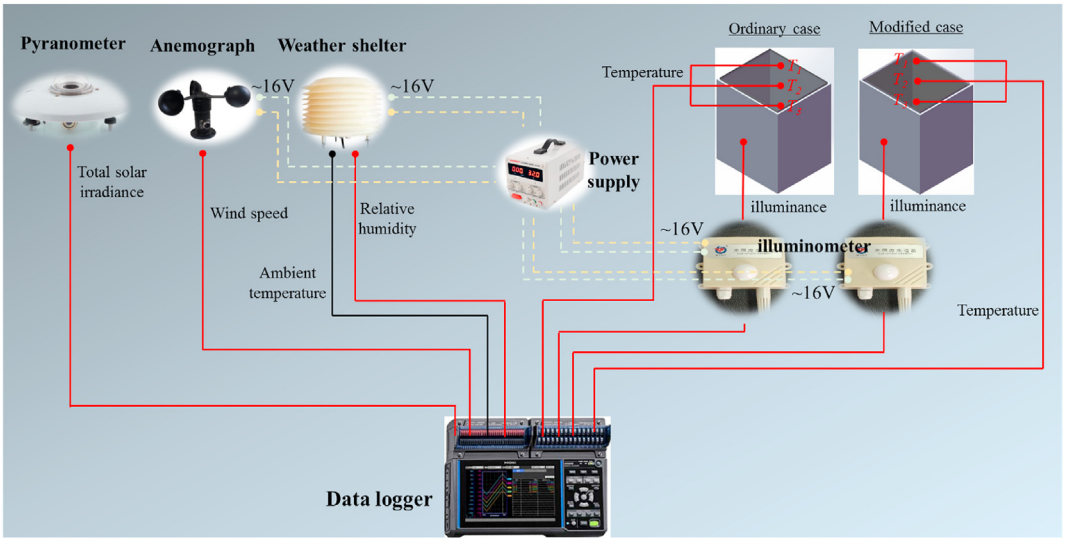

Fig. 4. Schematic of measuring setting system.

source (MAISHENG MS305D) with a voltage supply of 16 V. Furthermore, a pyranometer (TBQ-2) is used to measure the total irradiance and a weather shelter (HSTL-BYXWS) is applied to monitor the ambient temperature and relative humidity. The wind speed of the local air is tested by an anemograph (HSTL-FS01). Importantly, all data is automatically recorded using a data logger (HIOKI LR8450) with a time interval of 10 s. The list of experimental components is shown in Table 1.

2.3. Experimental results

The experimental tests were continuously conducted from 22:00 May 8th, 2021 to 22:00 May 9th, 2021. The temperature and illuminance results are shown in Fig. 5. The ambient parameters including solar irradiance (G, Wm^{-2}), wind speed (u_a, ms^{-1}), and relative humidity (RH, %) are presented in Fig. 5a. The indoor temperature inside the experiment box (T_1, T_2, T_3) and ambient temperature (T_a) are shown in Fig. 5b. From the results, it's clear that during the night period, the average air temperature inside two boxes is close, which are both lower than the ambient temperature and the difference value can be up to 4.1 °C. The main reason for this scenario is that the top glass is cooled passively by the radiative sky cooling due to its high thermal emissivity and this cooling effect is spread to the indoor air because of the convection and conduction heat transfer process between the indoor air and the glass. While during the daytime, the air temperature values inside the two boxes are both much higher than the ambient temperature. The comparison of the average air temperature inside two boxes is presented in Fig. 5c and it can be found that the modified case always shows lower indoor air temperature as compared with the ordinary case with the largest difference value of 16.4 °C, which proves that the ST/RC glass can regulate the thermal environment inside the building by adjusting the spectral characteristic of the glass. As illustrated in Fig. 2, the indoor air temperature can be governed by the ST/RC glass in three aspects as compared with the ordinary glass: (1) fewer visible light transmission into the building due to the relatively low visible transmittance of the ST solar film; (2) nearly no near-infrared solar radiation transmission into the building due to strong solar reflection within the near-infrared wavelength band; (3) strong heat emissive power due to the broad-band high emissivity of the ST/RC glass.

The internal illuminance of the two boxes is shown in Fig. 5d. Under the clear sky condition, the maximum internal illuminance of the ordinary case is 34,900 lx, which will add plenty of extra waste heat in the building and cause visual discomfort. On the contrary, with the use of the ST/RC glass, the inner illuminance can be decreased significantly as compared with the ordinary glass, and the illuminance in the modified case is only around 1/3 of that in the ordinary case, which indicates that the ST/RC glass can reduce the probability of glare, which will help to improve the daylighting environment and save the cooling energy at the same time.

Table 1
List of experimental components.

Device	Specification	Uncertainty
Pyranometer	TBQ-2	<5 %
Anemograph	HSTL-FS01	±0.2 m s^{-1}
Illuminometer	RS-GZ-V05-2	±7 %
Ambient temperature sensor	HSTL-BYXWS	±0.5 %
Relative humidity sensor	HSTL-BYXWS	±4.5 %
Thermocouple	Type T	±0.5 °C
Power supply	MAISHENG MS305D	/
Data logger	HIOKI LR8450	/

3. Large-scale modeling

3.1. Thermal analysis model

To further evaluate the feasibility of using light and thermal management of the glass for building energy saving under different weather conditions, a large-scale annual simulation was performed in this section. Here, the heat balance process of the glass with spectrally selective properties was analyzed and a schematic was shown in Fig. 6. There are several assumptions for this heat transfer model [30]: (i) the heat storage of the glass is neglected, (ii) the surface temperature of the glass is uniform, and (iii) the solar irradiance absorbed by the glass is apportioned equally to the outer and inner surface of the glass.

According to the first law of thermodynamic, the energy balance equations of the glass' outer and inner surface are presented as follows, respectively [30]:

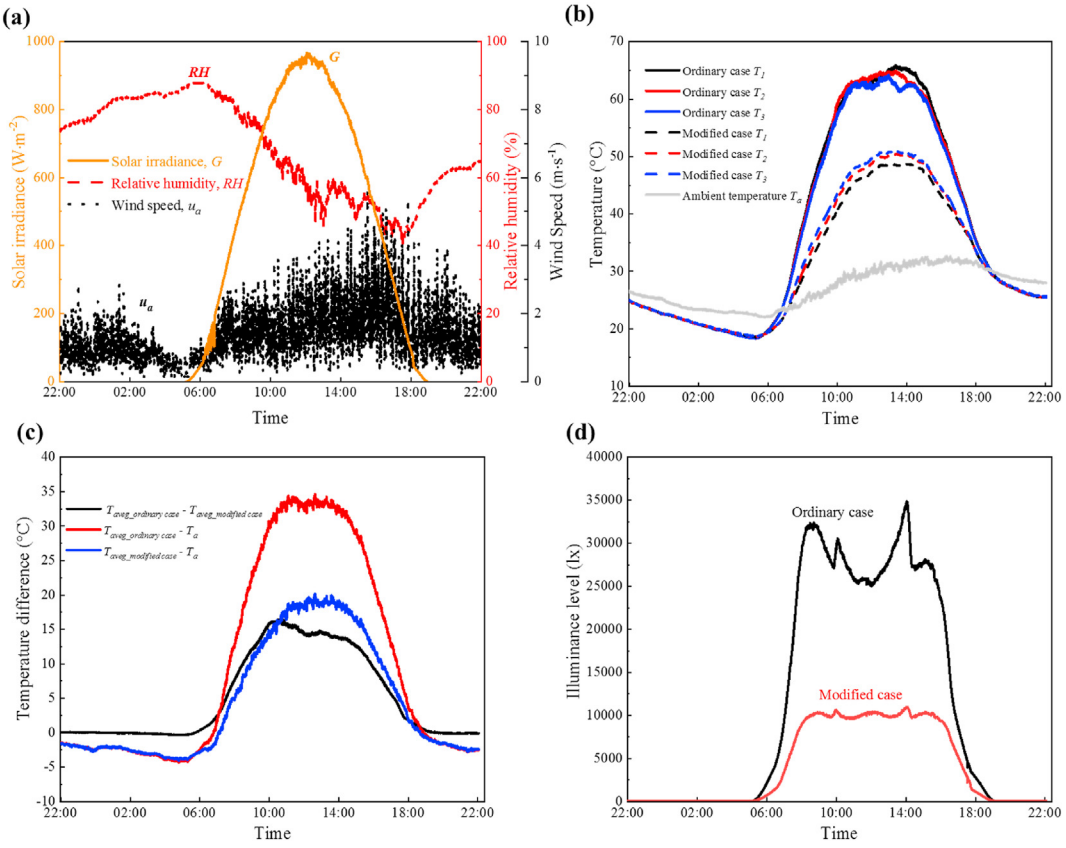

Fig. 5. (a) Measured solar irradiance, wind speed, and relative humidity during the testing period. (b) Measured indoor air temperature (T_1, T_2, and T_3) and ambient temperature. (c) The temperature difference among the indoor air temperature of the ordinary case, indoor air temperature of the modified case, and ambient air. (d) Measured illuminance level of ordinary case and modified case.

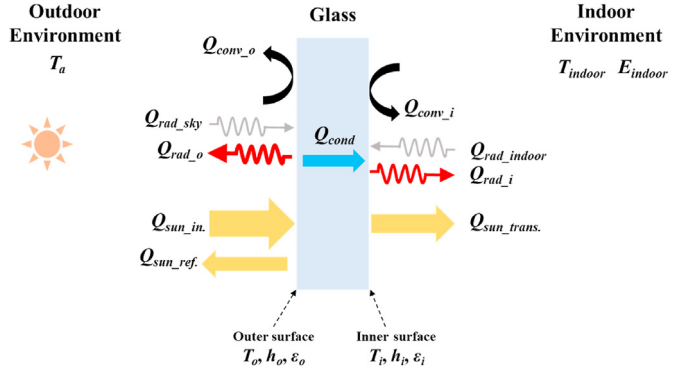

Fig. 6. Energy balance of the glass [30].

$$\begin{cases} Q_{rad\_sky} + Q_{sun\_o} - Q_{rad\_o} - Q_{cond} - Q_{conv\_o} = 0 \\ Q_{rad\_indoor} + Q_{sun\_i} - Q_{rad\_i} + Q_{cond} - Q_{conv\_i} = 0 \end{cases} \quad (1)$$

where Q_{rad_o} and Q_{rad_i} denote the thermal radiation power of the outer and inner surface, respectively. Q_{conv_o} and Q_{conv_i} denote the convection heat transfer power at the outer and inner surfaces, respectively. Q_{rad_sky} is the absorbed radiation power from the sky and Q_{rad_indoor} is the absorbed radiation power from the indoor environment. Q_{cond} is the heat conduction power from the outer surface to the inner surface. Q_{sun_o} and Q_{sun_i} denotes absorbed solar radiation at the outer and inner surface, respectively, which can be represented by Ref. [30]:

$$\begin{aligned} Q_{sun\_i} = Q_{sun\_o} &= \frac{1}{2}\left(Q_{sun\_in.} - Q_{sun\_ref.} - Q_{sun\_trans.}\right) \\ &= \frac{1}{2}\left(Q_{bm}cos\theta\alpha_{bm} + Q_{dif}\alpha_{dif}\right) \end{aligned} \quad (2)$$

where $Q_{sun\_in.}$, $Q_{sun_ref.}$and $Q_{sun_trans.}$denote the incident, reflected, and transmitted solar irradiance, respectively. Q_{bm} and Q_{dif} denote the beam normal and diffuse solar irradiance, respectively. α_{bm} and α_{dif} are solar absorptance of the glass for beam and diffuse solar irradiance, respectively. θ is the incident angle of the solar irradiance.

The thermal radiation power of the outer and inner surface can be expressed as [31]:

$$\begin{cases} Q_{rad\_o} = \varepsilon_o\sigma T_o^4 \\ Q_{rad\_i} = \varepsilon_i\sigma T_i^4 \end{cases} \quad (3)$$

where ε_o and ε_i denote the thermal emissivity of the outer and inner surfaces, respectively. T_o and T_i denote the temperature of the outer and inner surfaces, respectively. σ is the Stefan-Boltzmann constant.

The absorbed sky radiation and indoor long-wave radiation can be expressed as [31]:

$$\begin{cases} Q_{rad\_sky} = \varepsilon_o\varepsilon_{sky}\sigma T_a^4 \\ Q_{rad\_i} = \varepsilon_i E_{indoor} \end{cases} \quad (4)$$

where ε_{sky} denotes the effective emissivity of the sky. T_a is ambient temperature. E_{indoor} is the long-wave radiation power from the indoor environment.

The convection heat transfer power at the outer and inner surfaces can be expressed as [31]:

$$\begin{cases} Q_{conv\_o} = h_o(T_o - T_a) \\ Q_{conv\_i} = h_i(T_i - T_{indoor}) \end{cases} \quad (5)$$

where h_o and h_i denote the convection heat transfer coefficient at the outer and inner surfaces, respectively. T_{indoor} is the temperature of the indoor air.

The heat conduction power from the outer surface to the inner surface can be expressed as [31]:

$$Q_{cond} = k(T_o - T_i) \quad (6)$$

where k_o is the thermal conductance of the glass.

3.2. Building structure and glass spectrum configuration

As shown in Fig. 7a, a single house with the size of 30 m × 20 m × 10 m (length, width, and height) was simulated in the Maldives and this kind of house is widely used for public places, such as exhibition building [27]. The averaged daily ambient temperature and monthly solar radiation power in the Maldives are shown in Fig. 7b. The window-wall ratio of the roof glazing is close to 1, and its planar size is 29.9 m × 19.9 m (length and width). The materials of building envelopes are listed in Table 2. The *EnergyPlus* [32] that integrates the above thermal model is applied for simulation study in this section. During simulation, the temperature of the cooling setpoint is 26 °C, the working time of the air conditioner is 8:00–17:00, and the infiltration rate is set as 1/h throughout all days. Besides, a lighting mechanism is used for lighting behavior during the working time from 8:00 to 17:00. An illuminance value of 500 lx is set as the threshold value of illuminance. If the illuminance of the reference point is lower than the illuminance threshold value, the light is on and the lighting load is set as 9 W m^{-2}, otherwise, the light is off. The selected reference point is located in the center of the building and has a height of 1 m.

To fully explore the potential of glass with tailored spectral properties on the building energy saving, different spectral configurations of the glass were considered. The general idea to modify the glass is to add a spectrally selective coating (SSC) on the front surface of the ordinary glass (Clear glass, ID 103 in the International Glazing Database) [32] and the spectral properties of the SSC were configured from four wavelength regions that include ultraviolet (UV) region, visible (VIS) region, near-infrared (NIR) region, and mid-infrared (MIR) region. First, the SSC is set to be opaque within the ultraviolet region and near-infrared region. Second, the emissivity of the SSC within the mid-infrared region is set as 1. Third, a parameter called visible transmittance ratio (f) was used to evaluate the transmittance of the SSC within the visible region, which is defined as the ratio of transmittance of the SSC ($\tau_{SSC}(\lambda)$) to the ordinary glass ($\tau_{Ordinary\_glass}(\lambda)$) within the visible region and presented in the equation (1). The detailed spectral configurations of the SSC and glass with SSC were presented in Table 3 and Table 4, respectively, where τ, ρ, α, ε, λ represents the transmittance, reflectivity, absorptivity, emissivity, and wavelength.

$$f = \frac{\tau_{SSC}(\lambda)}{\tau_{Ordinary\_glass}(\lambda)} \quad (7)$$

The specific operation procedures of the simulation are as follows: First, the spectral properties (Table 3) of the SSC were input in *OPTICS* software. Second, in *OPTICS* software, the optical properties of the glasses with SSCs were calculated and read by the *WINDOW* software. Third, an IDF file that has the thermal and optical information of the glasses with SSCs can be exported by the *WINDOW* software. Finally, IDF files were imported to the *EnergyPlus* for calculation. The flow chart of the simulation process is presented in Fig. 8 for reference.

3.3. Validation of the simulation procedure

To validate the simulation procedure, the small-scale experimental cases described in the above section were selected as the validation objective. During the validation process, measured weather data that includes ambient temperature, wind speed, and relative humidity are used as input. Besides, dew point temperature was calculated based on the measured dry bulb ambient temperature and relative humidity [35], and the horizontal infrared radiation intensity was calculated using the effective sky emissivity that is obtained by an empirical correlation [36]. The calculated indoor air temperature was presented in Fig. 9 with the measured data plotted as reference. Notably, the measured data is the average temperature of the measured temperature of three thermocouples. It is clear that the simulated temperature agrees well with the experimental data, which indicates that the simulation procedure can be acceptable to simulate the large-scale condition.

3.4. Indoor temperature comparison

The indoor air temperature of the building under the OGC (see Table 4), MRGC, and MAGC was calculated and presented in Fig. 10. During simulation, the visible transmittance ratio f is set as 0.1 and

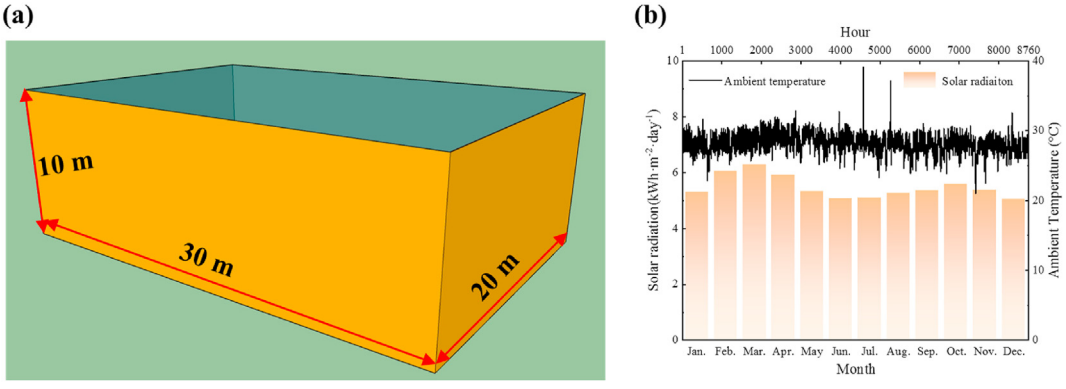

Fig. 7. (a) Schematic of the simulated building model. (b) Averaged daily ambient temperature and monthly solar radiation power in the Maldives [33].

Table 2
The thermophysical properties of the building envelop [32,34].

Envelope	Material (from outside to inside)	Thermal conductivity ($W \cdot m^{-1} \cdot K^{-1}$)	Density ($kg \cdot m^{-3}$)	Heat capacity ($J \cdot kg^{-1} \cdot K^{-1}$)
Wall	Brick (100 mm)	0.89	1920	790
	Air space (40 mm)			
	Brick (100 mm)	0.89	1920	790
Roof (wall, area fraction of 0.8 %)	Acoustic tile (20 mm)	0.06	368	590
	Air space (50 mm)			
	lightweight concrete (100 mm)	0.53	1280	840
Roof (glass, area fraction of 99.2 %)	glass	1.0	N.A.	N.A.
Floor	Insulation board (50 mm)	0.03	43	1210
	Heavyweight concrete (200 mm)	1.95	2240	900

Table 3
The detailed spectral configurations of the SSC.

Case name	UV region	VIS region	NIR region	MIR region
SSC-1	$\tau = 0$, $\rho = 1$	$\tau = f \cdot \tau_{Ordinary\_glass}(\lambda)$, $\rho = 1\text{-}f \cdot \tau_{Ordinary\_glass}(\lambda)$	$\tau = 0$, $\rho = 1$	$\varepsilon = 1$
SSC-2	$\tau = 0$, $\alpha = 1$	$\tau = f \cdot \tau_{Ordinary\_glass}(\lambda)$, $\alpha = 1\text{-}f \cdot \tau_{Ordinary\_glass}(\lambda)$	$\tau = 0$, $\alpha = 1$	$\varepsilon = 1$

Table 4
The detailed information of the glass with SSC.

Case name	Structure description
Ordinary glass case (OGC)	Ordinary glass + nothing
Modified reflective glass case (MRGC)	Ordinary glass + SSC-1
Modified absorptive glass case (MAGC)	Ordinary glass + SSC-2

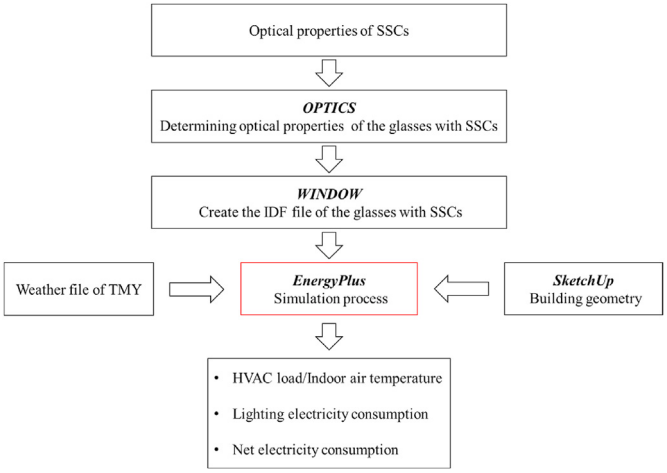

Fig. 8. The flow chart of the simulation process.

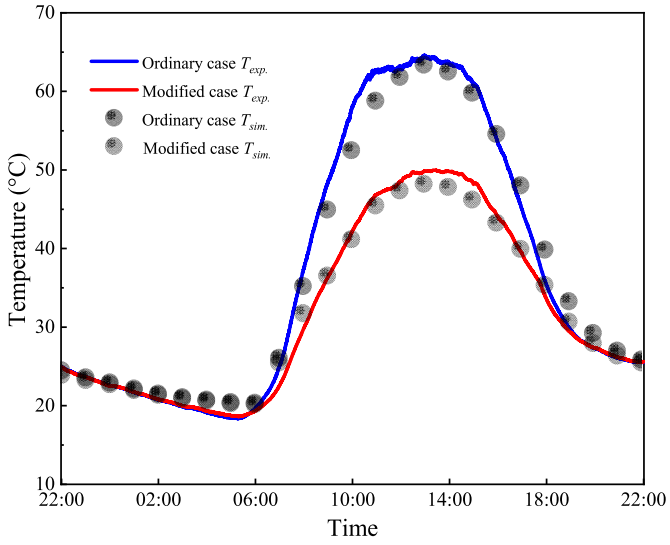

Fig. 9. Comparison of simulated and experimental indoor air temperature.

1, respectively, which represents the extreme condition for the glass. As shown in the figure, the daily averaged indoor air temperature under OGC is always highest and the indoor air temperature under MRGC or MAGC with $f = 0.1$ is always lowest. For example, the daily averaged indoor air temperature difference between the OGC and MRGC ranges from 4.5 °C to 13.5 °C with an average value of 9.7 °C. The main reason for the above results is that more sunlight transmits into the indoor environment and heats the indoor air under the OGC due to the high transmittance of the ordinary glass while the most of incident sunlight is blocked by the modified glass under the MAGC and MRGC even when the f equals 1. Besides, the high thermal emissivity of the glass in MRGC and MAGC improves the heat dissipation of the glass directly and the indoor air indirectly.

Fig. 11 shows the indoor air temperature difference between MAGC and MRGC under the f of 0.1 and 1. It can be seen that the indoor temperature under MAGC is always higher than that under MRGC and the temperature difference is more obvious when the $f = 0.1$. This is because the glass under MAGC absorbs more sunlight, which increases its temperature correspondingly, and this will heat the indoor air by convection and conduction heat transfer modes. So, the MAGC is the most effective condition to manage the indoor heat environment by adjusting the light and heat reaction among the glass, the sun, and the universe.

3.5. Energy-saving comparison

To further evaluate the effect of the light and thermal management of the glass on the energy saving of buildings, the cooling load of the building was calculated and presented in Fig. 12. There are three pieces of information inserted in the figure: (a) the cooling load of the building under OGC is always highest among the simulated cases, (b) the cooling load of the building under MAGC and MRGC decreases with the decreasing f, and (c) the cooling load of the building under MRGC is lower than that under MAGC when the f is the same. The above situations are the result of the light and thermal management of the glass. Specifically, a high reflection of the glass within the UV and NIR wavelength band can prevent

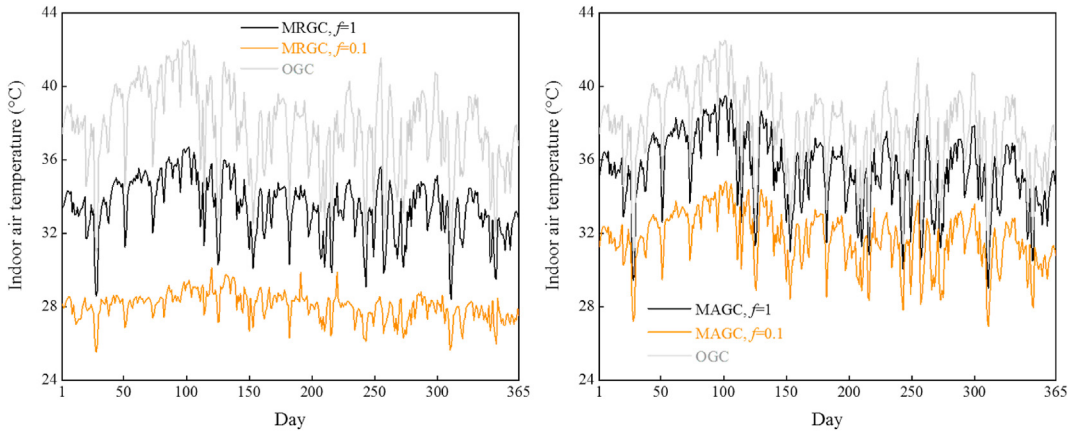

Fig. 10. Daily average indoor air temperature of the building under OGC, MRGC (f = 0.1 and 1), and MAGC (f = 0.1 and 1).

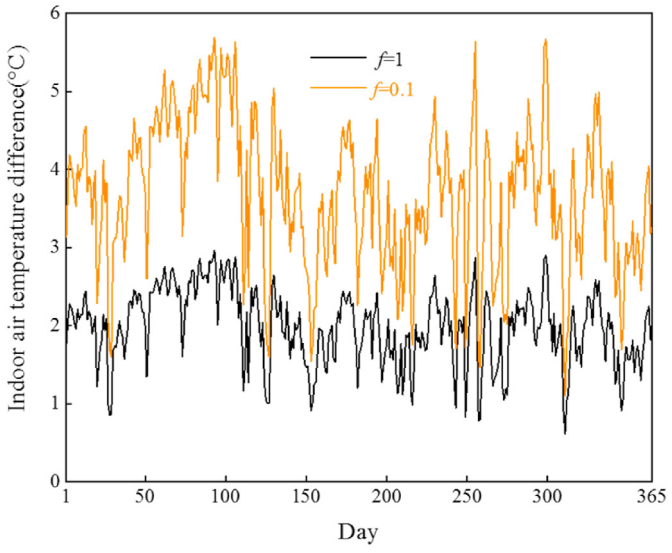

Fig. 11. Daily average indoor air temperature difference between the MAGC and the MRGC when f = 0.1 and 1.

nearly 50 % of sunlight and the unity thermal emissivity can improve the radiation heat transfer rate by approximately 16 %. Besides, a low and appropriate f can also block a large amount of sunlight, while maintaining the daylighting of the building at a reasonable and acceptable level.

To compare the cooling load of the building under MAGC and MRGC, the annual cooling load of the building under MAGC and MRGC with varying f is simulated and the results are plotted in Fig. 13a. It is clear that the annual cooling load of the building under MAGC is always higher than that under MRGC regardless of f. Besides, the annual cooling load difference of the building between the MAGC and MRGC enlarges with the decrease of the f, which means that the energy-saving performance of the MRGC is highlighted when the f is at a low level. For instance, the annual cooling load of the building under MRGC changes from 155.3 KWh·m^{-2} to 536.5 KWh·m^{-2} when f varies from 0.1 to 1, which are 256.8 KWh·m^{-2} and 115.5 KWh·m^{-2} lower than those under MAGC, corresponding to a relative reduction of approximately 62.3 % and 17.7 %, respectively.

Energy-saving of the building is the most important indicator to evaluate the feasibility of using light and thermal management of glass in buildings. Fig. 13b depicts the annual electricity saving of the buildings under MAGC and MRGC, the base objective is the electricity consumption of the building under OGC. The energy-saving of the building under MRGC is greater than that under

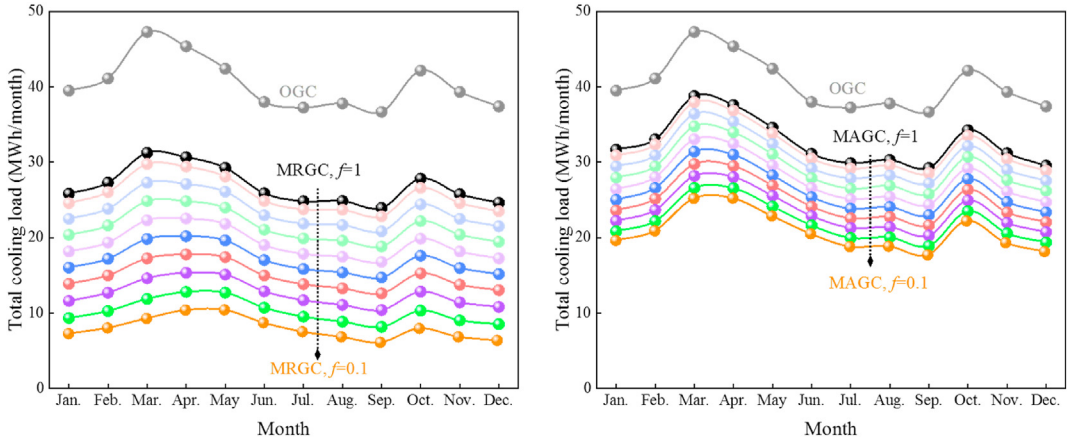

Fig. 12. Monthly cooling load of the building under OGC, MRGC (f = 0.1 to f = 1 with an interval of 0.1), and MAGC (f = 0.1 to f = 1 with an interval of 0.1).

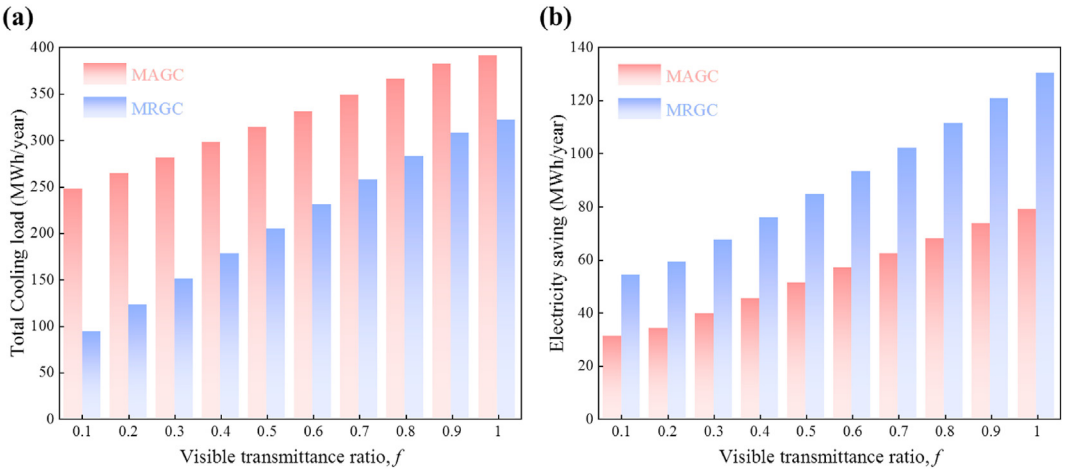

Fig. 13. (a) Annual cooling load of the building under MRGC and MAGC with different *f*. (b) Annual electricity saving of the building under MRGC and MAGC with different *f*.

MARC. When the *f* changes from 0.1 to 1, the energy saving of the building under MRGC varies from 54.1 MWh to 130.4 MWh with a near-linear trend, which can save electricity consumption by 66.5 % and 21 % compared with the base condition (i.e., OGC). Moreover, the energy saving of the building under MRGC is approximately 74.5 % and 65 % higher than that under MAGC, showing great potential for light and thermal management of buildings. Importantly, simulation results show the illuminance of the reference point is always higher than the illuminance threshold value even when the *f* is 0.1, so the light is always off, which means that there is no lighting consumption in the case and the electricity-saving shown in Fig. 11b is only related to the electricity-saving from space cooling. There are two main reasons for the above scenario, the first is that the selected building has a glass roof so that the more visible light can transmit into the building, the second is that the Maldives has abundant solar resources so that more visible light can potentially be used. If the different types of building structure and meteorological data are used for simulation, the lighting consumption will possibly occur. In these conditions, the net electricity saving that includes the effect of space cooling/heating and lighting is the objective function to evaluate the energy-saving performance of the proposed strategy. Besides, the effect of different climate conditions, building structures, and the location of the glass on the spectral properties modification of the glass can be further explored in the future so that the idea of light and thermal management of glass for building energy saving can be extended to different conditions and the energy-saving potential can be maximally explored.

4. Conclusions

In this paper, a semi-transparent radiative cooling (ST/RC) glass is proposed to reduce the energy consumption for cooling in buildings by managing the radiative properties of the glass. Comparative outdoor experiments were performed to preliminarily evaluate the performance of the ST/RC glass for energy saving of building. Besides, large-scale modeling was conducted to predict the energy-saving performance of buildings based on glass with different radiative properties. The important conclusions are presented as follows:

(1) The proposed ST/RC glass has selective transmission within the visible light region and exhibits strong reflectivity within the near-infrared wavelength band. Besides, the ST/RC glass has a high thermal emissivity which is better than that of ordinary glass.
(2) The indoor air temperature of the small box with the ST/RC glass is lower than that with the ordinary glass with a maximum temperature reduction of 16.4 °C, while the daylighting level of the small box with the ST/RC glass can be maintained at a more reasonable level.
(3) The energy saving of buildings under MRGC is approximately 21%–66.5 %, indicating the strategy of using light and thermal management of glass has the potential to reduce the energy consumption of the buildings.

In summary, this work proposes a novel strategy to reduce the energy consumption of buildings, especially in hot climate regions, by selective utilization of sunlight and enhancement of radiative cooling, which provides a guide for the design of energy-saving windows.

Credit author statement

Bin Zhao: Project administration, Performed the experiments, Data curation, Formal analysis, Writing – original draft, Writing – review & editing, Funding acquisition, conceived the idea and supervised the project; **Chuyao Wang**: Performed the simulation and data analysis, Writing – review & editing; **Mingke Hu**: Data analysis, Writing – review & editing; **Xianze Ao**: Performed spectral testing, Formal analysis; **Jie Liu**: Performed spectral testing; **Qingdong Xuan**: Performed the experiments, Data curation, Formal analysis, Writing – original draft, Writing – review & editing, Funding acquisition; **Gang Pei**: Project administration, Writing – review & editing, conceived the idea and supervised the project; Funding acquisition.

Declaration of competing interest

The authors declare that they have no known competing financial interests or personal relationships that could have appeared to influence the work reported in this paper.

Acknowledgments

This work was supported by the National Key R&D Program of China (2018YFB1900602), the National Natural Science Foundation of China (NSFC 51776193), Project funded by China Postdoctoral

Science Foundation (2020TQ0307 and 2020M682033), and Fundamental Research Funds for the Central Universities (WK2090000028, WK5290000001, JZ2021HGQA0234, and JZ2021HGTA0153).

References

[1] Zhao B, Hu M, Ao X, Pei G. Conceptual development of a building-integrated photovoltaic–radiative cooling system and preliminary performance analysis in Eastern China. Appl Energy 2017;205:626–34.
[2] Li X, Sun B, Sui C, Nandi A, Fang H, Peng Y, et al. Integration of daytime radiative cooling and solar heating for year-round energy saving in buildings. Nat Commun 2020;11:6101.
[3] Li X, Zhou Y, Yu S, Jia G, Li H, Li W. Urban heat island impacts on building energy consumption: a review of approaches and findings. Energy 2019;174:407–19.
[4] Chen J, Lu L, Gong Q, Wang B, Jin S, Wang M. Development of a new spectral selectivity-based passive radiative roof cooling model and its application in hot and humid region. J Clean Prod 2021;307:127170.
[5] Zhao B, Hu M, Ao X, Chen N, Pei G. Radiative cooling: a review of fundamentals, materials, applications, and prospects. Appl Energy 2019;236:489–513.
[6] Zhai Y, Ma Y, David SN, Zhao D, Lou R, Tan G, et al. Scalable-manufactured randomized glass-polymer hybrid metamaterial for daytime radiative cooling. Science 2017;355:1062–6.
[7] Raman AP, Anoma MA, Zhu L, Rephaeli E, Fan S. Passive radiative cooling below ambient air temperature under direct sunlight. Nature 2014;515:540–4.
[8] Zhao D, Aili A, Zhai Y, Xu S, Tan G, Yin X, et al. Radiative sky cooling: Fundamental principles, materials, and applications. Appl Phys Rev 2019;6:021306.
[9] Gentle AR, Dybdal KL, Smith GB. Polymeric mesh for durable infra-red transparent convection shields: applications in cool roofs and sky cooling. Sol Energy Mater Sol Cells 2013;115:79–85.
[10] Gentle AR, Smith GB. A subambient open roof surface under the mid-summer sun. Adv Sci 2015;2:1500119.
[11] Boixo S, Diaz-Vicente M, Colmenar A, Castro MA. Potential energy savings from cool roofs in Spain and Andalusia. Energy 2012;38:425–38.
[12] Li X, Peoples J, Yao P, Ruan X. Ultrawhite $BaSO_4$ paints and films for remarkable daytime subambient radiative cooling. ACS Appl Mater Interfaces 2021;13:21733–9.
[13] Li X, Peoples J, Huang Z, Zhao Z, Qiu J, Ruan X. Full daytime sub-ambient radiative cooling in commercial-like paints with high figure of merit. Cell Reports Phys Sci 2020;1:100221.
[14] Mandal J, Yang Y, Yu N, Raman AP. Paints as a scalable and effective radiative cooling technology for buildings. Joule 2020;4:1350–6.
[15] Ao X, Hu M, Zhao B, Chen N, Pei G, Zou C. Preliminary experimental study of a specular and a diffuse surface for daytime radiative cooling. Sol Energy Mater Sol Cells 2019;191:290–6.
[16] Shen H, Tan H, Tzempelikos A. The effect of reflective coatings on building surface temperatures, indoor environment and energy consumption—an experimental study. Energy Build 2011;43:573–80.
[17] Salameh T, Assad MEH, Tawalbeh M, Ghenai C, Merabet A, Öztop HF. Analysis of cooling load on commercial building in UAE climate using building integrated photovoltaic façade system. Sol Energy 2020;199:617–29.
[18] Javanroodi K, Mahdavinejad M, Nik VM. Impacts of urban morphology on reducing cooling load and increasing ventilation potential in hot-arid climate. Appl Energy 2018;231:714–46.
[19] Zeng J, Wang Y, Rajan K, Xiao Z, Rehman Sagar RU, Liu P. Transparent-to-black electrochromic smart windows based on N, N, N′, N′-Tetraphenylbenzidine derivatives and tungsten trioxide with high adjustment ability for visible and near-infrared light. Sol Energy Mater Sol Cells 2021;226:111070.
[20] Nundy S, Mesloub A, Alsolami BM, Ghosh A. Electrically actuated visible and near-infrared regulating switchable smart window for energy positive building: a review. J Clean Prod 2021;301:126854.
[21] Chambers J, Hollmuller P, Bouvard O, Schueler A, Scartezzini J-L, Azar E, et al. Evaluating the electricity saving potential of electrochromic glazing for cooling and lighting at the scale of the Swiss non-residential national building stock using a Monte Carlo model. Energy 2019;185:136–47.
[22] Oh S-W, Kim S-H, Baek J-M, Yoon T-H. Optical and thermal switching of liquid crystals for self-shading windows. Adv Sustain Syst 2018;2:1700164.
[23] Abundiz-Cisneros N, Sanginés R, Rodríguez-López R, Peralta-Arriola M, Cruz J, Machorro R. Novel Low-E filter for architectural glass pane. Energy Build 2020;206:109558.
[24] Somasundaram S, Chong A, Wei Z, Thangavelu SR. Energy saving potential of low-e coating based retrofit double glazing for tropical climate. Energy Build 2020;206:109570.
[25] Jelle BP, Kalnæs SE, Gao T. Low-emissivity materials for building applications: a state-of-the-art review and future research perspectives. Energy Build 2015;96:329–56.
[26] Somasundaram S, Thangavelu SR, Chong A. Improving building efficiency using low-e coating based retrofit double glazing with solar films. Appl Therm Eng 2020;171:115064.
[27] Yi Z, Lv Y, Xu D, Xu J, Qian H, Zhao D, et al. Energy saving analysis of a transparent radiative cooling film for buildings with roof glazing. Energy Built Environ 2021;2:214–22.
[28] Zhu L, Raman A, Wang KX, Anoma MA, Fan S. Radiative cooling of solar cells. Optica 2014;1:32–8.
[29] Zhu L, Raman AP, Fan S. Radiative cooling of solar absorbers using a visibly transparent photonic crystal thermal blackbody. Proc Natl Acad Sci Unit States Am 2015;112:12282–7.
[30] US Department of Energy. Engineering reference. EnergyPlus™ version 8.7 documentation.
[31] Bergman TL, Lavine AS, Incropera FP, DeWitt DP. Fundamentals of heat and mass transfer. Seventh. John Wiley & Sons; 2011.
[32] EnergyPlus. https://www.energyplus.net/.
[33] Weather data. https://energyplus.net/weather.
[34] Ng PK, Mithraratne N, Kua HW. Energy analysis of semi-transparent BIPV in Singapore buildings. Energy Build 2013;66:274–81.
[35] Li W, Dong M, Fan L, John JJ, Chen Z, Fan S. Nighttime radiative cooling for water harvesting from solar panels. ACS Photonics 2021;8:269–75.
[36] Zhao B, Pei G, Raman AP. Modeling and optimization of radiative cooling based thermoelectric generators. Appl Phys Lett 2020;117:163903.